A 2.45 GHz Smart Antenna for Location-Aware Single-Anchor Indoor Applications

A. Cidronali, S. Maddio, G. Giorgetti[†], I. Magrini, S. K. S. Gupta[†] and G. Manes

Dept. of Electronics and Telecomm., University of Florence, I-50139 Florence, ITALY; e-mail: *first.last*@unifi.it
[†]IMPACT Lab, Arizona State University, Tempe, AZ 85287, USA; e-mail: *first.last*@asu.edu

Abstract—**This paper proposes a new switched beam array optimized for 2.45 GHz wireless indoor applications. The antenna supports directional communication to enable spatial reusability, and polarization diversity to mitigate multipath propagation. It also supports absolute 2D target localization using measurements from a single anchor node. The paper describes the antenna design, the implementation and the experimental characterization, along with its positioning applications. The localization results obtained with data collected from indoor measurements, showing an average localization error as low as 1.7 m.**

Index Terms—**Indoor communications, wireless localization, pointing diversity, polarization diversity, microstrip antenna.**

I. INTRODUCTION

THE Smart Antenna (SA) is an emerging technology that is effective in improving the performance of wireless networks. The ability to reconfigure some of their parameters such as the radiation pattern and polarization improves the link quality and enables spatial reusability, thus having a positive impact in terms of reliability and network capacity.

There is a large consensus that SAs could be beneficial in implementing current and future mobile and context-aware indoor applications; although, specific commercial applications of SAs are still to come. Indoor applications are challenged by multipath propagation, and interferences are more likely to occur due to the large number of devices sharing a confined space. The problem is further aggravated by the frequency overlaps between popular standards such as WiFi, Bluetooth and Zigbee. Additionally, many indoor applications are expected to sense the user's position to implement *context-aware* services that facilitate access to nearby resources, deliver location sensitive information, and enforce proximity based security policies. To this regard, indoor positioning has been actively investigated in recent years, and numerous approaches have been proposed in the literature [4], [8].

We propose a switched beam antenna designed to address the challenges of indoor applications. The antenna is intended to augment a wireless devices operating as coordinator or *Base Station* (BS), and its design has been optimized for installation on the ceiling of any large indoor space (see Fig. 1). This position is unobtrusive to the users, and it allows placement in the center of the space, the preferred location for a BS required to serve several nodes. The antenna is implemented by combining six faces pointing in different directions. By switching between different faces, the BS can establish preferred communication with groups of devices
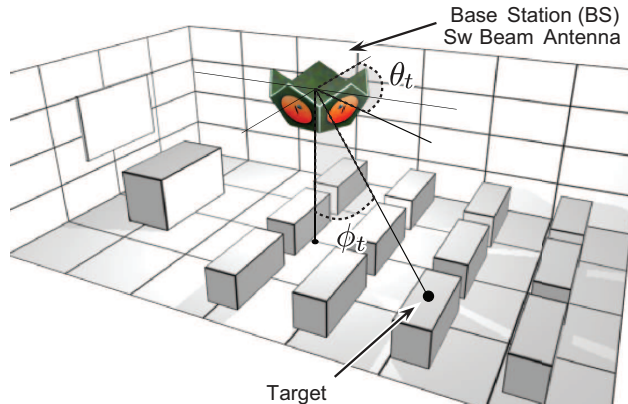
Fig. 1.   Application scenario for the proposed smart antenna.

located in the area illuminated by each antenna, thus reducing the probability of interferences in dense networks.

The antenna is also designed to support indoor positioning. Thanks to the 3D arrangement of the antenna faces, the system can locate a target by estimating both the azimuth θ_t and elevation ϕ_t *Direction of Arrival* (DOA) of the incoming messages. This approach implements a *single-anchor* positioning system that requires *zero-configuration*; therefore it is suitable for low-cost deployments, ad-hoc applications (e.g. emergency response), and other scenarios where installing a network of anchors is not desirable or feasible.

Section II describes the design principles and implementation details for the proposed antenna at 2.45 GHz, although this frequency band doesn't rapresent a limit to the operative principle; the measurements of some of its characteristic parameters are reported in Section III. In Section IV we discuss the use of the antenna in indoor positioning applications; we also report localization results obtained using RSS trances from an indoor application.

II. SWITCHED BEAM ARRAY ANTENNA

The design principles for the antenna respond to the need of implementing a steerable beam capable of selectively illuminating the space underneath the BS and collect information useful for target localization. While the single beams should exhibits a directional pattern to reduce the interferences and enable spatial reusability, the cumulative radiation pattern should be almost isotropic to ensure reliable communications with users at arbitrary locations. The antenna should be able
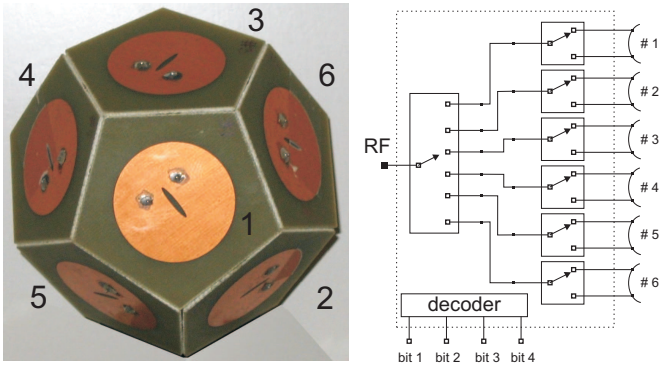
Fig. 2. Prototype of the switched beam antenna (left); schematic diagram of the elements' feeding structure (right).

Fig. 3. Elliptical slit disc antenna on pentagonal ground prototype (left), quotes are in mm (right); substrate: FR4, 1.6 mm thickness, 17 μm copper thickness. The antenna element feeding circuitry based on SPDT switch.

to operate in circular polarization to mitigate indoor multipath propagation; additionally, the signals received by the various antenna elements need to be angularly decorrelated to enable target localization based on DOA estimation.

To meet the design requirements, we have identified the class of *platonic solids* as a suitable geometry for the antenna implementation; in particular, the proposed solution is an antenna shaped as a dodecahedron (see Fig. 2). Since the 3D arrangement of the six pentagonal elements covers almost half of the whole solid steradian, this antenna geometry is suitable for a base station installed on the ceiling of a room and required to support directional communication with devices underneath it.

The antenna polarization and pointing diversity mechanism is enabled by selecting one out of the six radiative elements, each of them capable to operate in either left-hand or right-hand circular polarization (LH/RHCP). The antenna signal distribution network is represented schematically in Fig. 2 (right). The switched beam solution implemented by a multiplexing circuit is the result of a trade-off between the need of a simple architecture and a wide steerable beam angle.

A. Array Element

Platonic solids have *identical faces* and *identical dihedral angles*; therefore the six antenna elements have identical characteristics and can be manufactured with limited costs. Each element is a microstrip patch antennas printed over a plastic substrate shaped in a pentagonal geometry. In this case, an appropriate shape for the radiator in term of filling factor is a disc. A canonical disc patch antenna working in the fundamental TM_{11} mode exhibits a mono-lobe radiation pattern characterized by an half power angle of about $50°-60°$. Being the dihedral angle of the dodecahedron $\sim 116°$, the use of this kind of patch meets the requirements of having a cumulative radiation with an (approximately) uniform coverage.

Antenna capable of operating in CP have proven useful in reducing multipath propagation [5], [9], and for improving indoor localization results [7]. In our case the CP radiation is achieved by a proper mode perturbation at the center of the disk that splits the fundamental mode in two degenerated ones. The resultant quasi-symmetrical shape can sustain two geometrically orthogonal linearly polarized and frequency overlapping modes. By appropriate placement of the probe in an intermediate position between the axes of the two detuned modes, the generated fields combine in quadrature generating a CP far-field.
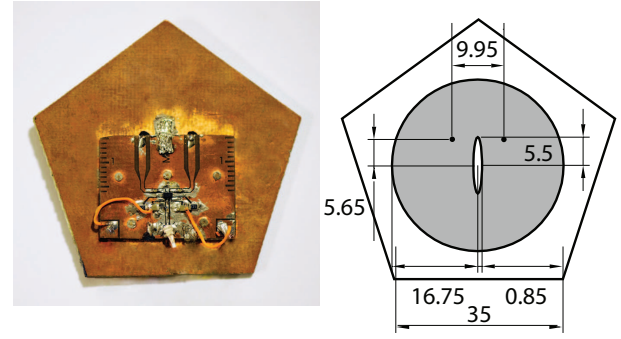
Our prototype was designed on FR4 substrate ($\epsilon_r = 4.4$, $h = 1.6$ mm) with a concentric ellipse serving as a perturbation shape. We traded off dimension and performance to be the most compact possible. The ground plane of each antenna element was taken only slightly larger than the patch resonator dimension, although its limited extension leads to unavoidable coupling among the antennas. Figure 3 (right) shows the final design, which was optimized by numerical analysis conducted with a commercial full-wave CAD. The patch central symmetry allows two possible feed positions, and, in turn, the excitation of RHCP or LHCP.

B. Polarization Diversity Control

The antenna CP diversity is achieved by means of a single-pole double-throw (SPDT) switch connected between the two feeds points and the antenna element input. The selection of the proper pin determines which polarization is activated.

Since the whole CP mechanism is ruled by a degeneration condition, it is mandatory to preserve the modal current density. This means that alternatively the terminating impedance should be either 50 Ω or an open circuit. A real SPDT cannot provide an exact open circuit for the off-state pin; therefore we compensated for the non-ideality of the device by tuning the electrical length of the transmission line between the SPDT and the antenna feeder.

The insertion of the SPDT introduce a loss that decreases the overall antenna gain. To minimize such loss, we adopted the Skyworks AS179 reflective switch that exhibits a nominal 0.4 dB insertion loss and more than 20 dB of isolation. The PCB with the CP diversity selector circuit is assembled on the rear face of the antenna as shown in Fig. 3(left). The same figure also shows the transmission lines of proper length, the SPDT, and the miniaturized coaxial connector used to interface the dual CP antenna to the antenna selector.

Figure 4 shows the input impedance of the antenna prototype in the two polarization states. The two cuspids around the center frequency, which are effects of the mode degeneration,
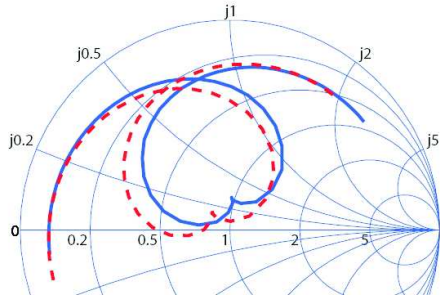
Fig. 4. Measured antenna element matching, in the two CP states between 2.3 to 2.6 GHz; RHCP continous line, LHCP dashed line. The data are measured at the SPDT input port

reflects the generation of the CP. The experimental characterization of the CP quality exhibited an axial ratio less than 5 dB with a phase error less than 5 degree in a 60 MHz bandwidth about 2.45 MHz.

C. Beam Diversity Control

The beam selection for antenna developed in this work is implemented using a single-pole six-through switch (SP6T). A schematic representation of the signal distribution architecture is reported in Fig. 2(right). The patch selection is controlled by three bits, while one bit selects the CP mode. This bit is common to all the SPDT on the back of the antenna elements.

Our antenna prototype adopts the HMC252QS24 GaAs SP6T non-reflective switch, which exhibits a nominal insertion loss of 1.5 dB and an isolation in excess of than 30 dB at 2.45 GHz. The adoption of this kind of switch minimizes the interaction between elements. In fact, the matched loads connected to the idle antennas permits to dissipate the signal interaction between elements rather than reirradiate it back, thus resulting in a minimal corruption of the pattern when compared to the isolated element case.

III. CHARACTERIZATION MEASUREMENT OF THE SWITCHED SIX-BEAMS ANTENNA

We measured the radiation patterns in an anechoic chamber by mounting the prototype on a computer controlled antenna rotor. The measurements collected at a frequency of 2.45 GHz are organized against a reference system in which the angle $\phi = 0°$ is defined by the axis of the antenna #1, while θ is the azimuthal angle with its zero at the junction of antenna elements #2 and #5. (see Fig. 1 and 2).

The first set of data measured for $\phi = 90°$ is reported in Fig. 5. (note that this elevation angle is not the one with maximum radiation). The graphs show that the combined radiation spans the entire 2π angle, with the single beam irradiating in five equally spaced sectors. The patterns' slight asymmetries are due to the corresponding geometry asymmetries arised from the arrangement of the antenna elements, the fabrication uncertainty, and the interaction with the control electronics surrounding the prototype during the measurements.

When the control units selects the #1 antenna element, as expected, the pattern resembles that of an omnidirectional antenna, and for this elevation angle the radiation pattern has a comparable lower magnitude. The switched beam antenna
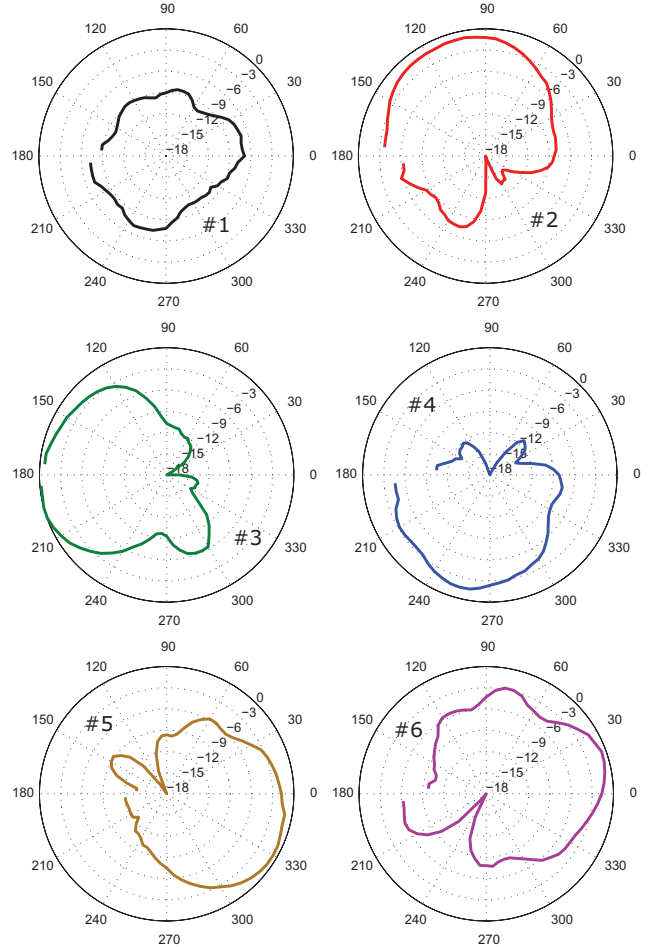
Fig. 5. Radiation patterns corresponding to the six antenna states in LHCP measured for $\phi = 90°$ and θ ranging from $-175°$ to $175°$.
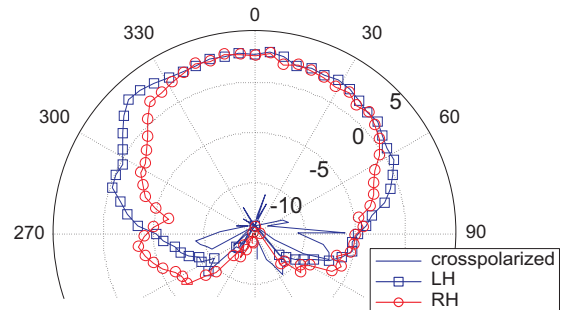
Fig. 6. Gain patterns of element #1 in LHCP, RHCP and crosspolarization measured for $\theta = 0°$ and ϕ ranging from $-175°$ to $175°$.

gain patterns for $\theta = 0°$ and antenna element #1 activated in both the polarizations are reported in Fig. 6. From the graphs is observed maximum for $\phi = 0°$ for both the LHCP and RHCP, which is the direction toward the floor in the operative conditions. This graph also reports the gain measured in crosspolarization condition. From the graphs we can read the gain at $\phi = 0°$, which is 1.46 dB and 1.87 dB respectively for the RHCP and LHCP.

To characterize the ability to reject multipath interferences, we have measured the transmission link parameter in two configurations with a pair of antennas operating in either copolarization and cross-polarization. The result of the comparison is reported in Fig. 7 for the frequency range from 2.3 to
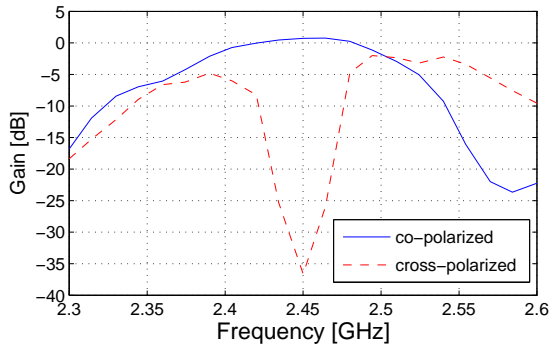
Fig. 7. Transmission coefficeints for co-polarized and cross-polarized links,for antenna element #1 for $\theta = 0°$ and $\phi = 0°$.

2.6 GHz. From the graph, where the link losses are removed, it is evident a deep minimum at 2.45 GHz, lower than -35 dB. In operative conditions, this figure is important because it reflects the capability to reject multipath signal. The input matching, not reported here, ranges from -25 to -13 dB at 2.45 GHz for the two polarizations.

IV. 2D TARGET LOCALIZATION EXPERIMENT

One of the key element of the proposed solution is its ability to compute the 2D position of users in the deployment space. This feature is enabled by implementing a protocol where the user's device exchanges messages with the six antenna elements.

According to the Friis' equation, the received power depends on the target's distance and the antenna gain $G_i(\phi_t, \theta_t)$ of each face i, where the pair of angles (ϕ_t, θ_t) defines the DOA of the target's messages (see Fig. 1). Given the small antenna dimensions, all the antenna elements are at about the same distance from the target; therefore, the differences in received power (in dB) between two elements i and j will only depend on their gains: $P_i - P_j = G_i(\phi_t, \theta_t) - G_j(\phi_t, \theta_t)$.

Once the RSS measurements have been collected, the DOA of the messages tranmitted by the target can be estimated via *array signal processing* algorithms [3]. Our implementation uses the *Multiple Signal Classification* (MUSIC) approach, which applies spectral decomposition to the covariance matrix of the power readings on each antenna element to produce an estimated DOA. After the pair of angles $(\hat{\phi}_t, \hat{\theta}_t)$ have been estimated, the user position on the plane underneath the antenna can be computed by applying trigonometric functions.

Notably, this approach improves over RSS ranging techniques that requires knowledge of the propagation model parameters and need measurements from three anchor nodes. This approach also extends previous solutions exploiting beacons with directional antennas located on the target's plane [1], [6], which requires two anchors for absolute 2D localization.

We have evaluated the localization results in a *proof-of-concept* application implemented in a large classroom with rows of desks and chairs [2]. The RSS traces were collected on a 6×4 grid measuring $7.2\,\text{m} \times 8\,\text{m}$. In addition to the DOA estimation approach, we also evaluated two other algorithms. The first of them estimates the target position by identifying the face that receives the maximum RSS. Since the faces illuminate different areas of the room, the target can be approximately located in center of the area covered

TABLE I
EXPERIMENTAL LOCALIZATION RESULTS

Algorithm	Avg. Error [m]
DOA Estimation (MUSIC)	1.69
Strongest RSS	2.34
Fingerprinting	2.32

by the antenna element with strongest reception. The third localization approach uses a *fingerprinting* technique [4] that creates an RF-map of the room using RSS measurements from the six antenna elements. Table I shows the localization results evaluated on the 6×4 grid. A more detailed description of the application scenario and the localization techniques is presented in [2].

V. CONCLUSIONS

We have introduced a new smart antenna based on the concept of switched beam and circular polarization diversity capable of operating with IEEE 802.1x.y wireless devices in the 2.45 GHz band. We have described in detail the design approach and validated experimentally a prototype fabricated in FR4 and COTS semiconductor switches. The proposed solution also show that single-anchor 2D localization is feasible using a low-cost system that requires zero-configuration. Indoor measurements have shown satisfactory localization results using different localization algorithms. Using array signal processing algorithms, we have achieved an average localization error as low as $1.7\,\text{m}$, making the system suitable for fine-grained indoor positioning.

REFERENCES

[1] J. Ash and L. Potter. Sensor network localization via received signal strength measurements with directional antennas. *Proc. of the Allerton Conf. on Communication, Control, and Computing*, 2004.

[2] G. Giorgetti, A. Cidronali, K. Gupta, and G. Manes. Single-anchor indoor localization using a switched-beam antenna. *Communications Letters, IEEE*, Vol. 13, Jan. 2009, pp. 58-60.

[3] H. Krim, M. Viberg, and C. MIT. Two decades of array signal processing research: the parametric approach. *Signal Processing Magazine, IEEE*, 13(4):67–94, 1996.

[4] H. Liu, H. Darabi, P. Banerjee, and J. Liu. Survey of Wireless Indoor Positioning Techniques and Systems. *IEEE Trans. On Systems Man And Cybernetics*, 37(6):1067, 2007.

[5] T. Manabe, Y. Miura, and T. Ihara. Effects of antenna directivity and polarization on indoor multipath propagation characteristics at 60 ghz. *IEEE Journal on Selected Areas in Comm.*, 14(3):441–448, 1996.

[6] D. Niculescu and B. Nath. VOR base stations for indoor 802.11 positioning. *MobiCom'04*, pages 58–69, 2004.

[7] R. Szumny, K. Kurek, and J. Modelski. Attenuation of multipath components using directional antennas and circular polarization for indoor wireless positioning systems. *European Microwave Conference, 2007*, pages 1680–1683, Oct. 2007.

[8] M. Vossiek, L. Wiebking, P. Gulden, J. Wieghardt, C. Hoffmann, P. Heide, S. Technol, and G. Munich. Wireless local positioning. *Microwave Magazine, IEEE*, 4(4):77–86, 2003.

[9] F. Yildirim, A. Sadri, and H. Liu. Polarization effects for indoor wireless communications at 60 ghz. *Communications Letters, IEEE*, 12(9):660–662, September 2008.